

# Pressure Sensors of CVD Diamond Films

Makoto Kitabatake and Masahiro Deguchi

Central Research Laboratories, Matsushita Electric Industrial Co., Ltd.,  
3-4 Hikaridai, Seika-cho, Soraku-gun, Kyoto 619-02, Japan

(Received March 13, 1998; accepted July 30, 1998)

**Key words:** p-type diamond films, chemical vapor deposition, piezoresistive effect, gauge factor

Electrical and piezoresistive properties of chemical-vapor-deposited boron-doped (B-doped) p-type polycrystalline diamond films are investigated. The diamond films about 2  $\mu\text{m}$  thick were grown on a flat insulating polycrystalline diamond substrate using a conventional microwave plasma CVD system. Deposition conditions for the diamond films were carefully selected to suppress the degradations, such as the surface conductive layer, the impurity-band conduction under high B-doping concentration, and the resistive conduction across the grain boundaries. The optimized film exhibits hole conduction originated from B acceptor with an activation energy of 0.31–0.33 eV and reasonably high mobility ( $> 30 \text{ cm}^2/\text{V}\cdot\text{s}$  at 300 K). A piezoresistor (500  $\mu\text{m}$  long and 50  $\mu\text{m}$  wide) of the p-type polycrystalline diamond film was fabricated on a diaphragm structure using photolithography and reactive ion etching in an oxygen plasma. Relative change of the electrical resistance ( $R/R_0$ ) of the p-type diamond piezoresistor is almost proportional to the applied strain. Gauge factor  $K$  for the p-type diamond piezoresistor is derived to be  $\sim 1,000$  at room temperature and  $> 700$  at 200°C.

## 1. Introduction

Diamond is one of the most promising materials for new semiconductor devices because of its unique electrical and mechanical properties, such as wide band gap ( $E_g \sim 5.5 \text{ eV}$ ), high electrical breakdown field ( $3.5 \times 10^6 \text{ V/cm}$ ),<sup>(1)</sup> high hole mobility ( $> 1,200 \text{ cm}^2/\text{V}\cdot\text{s}$ ),<sup>(2)</sup> high thermal conductivity ( $\sim 20 \text{ W/cm}\cdot\text{K}$ ),<sup>(3)</sup> and high Young's modulus ( $E \sim 1 \times 10^{12} \text{ N/m}^2$ ).<sup>(4)</sup> Rapid advances in the synthesis techniques of diamond films, for example microwave plasma chemical vapor deposition (CVD),<sup>(5–7)</sup> enabled a wide variety of applications of diamond to develop. The semiconducting CVD diamond thin film is

suitable for sensors, such as radiation detectors,<sup>(8)</sup> photosensors,<sup>(9)</sup> thermistors,<sup>(10,11)</sup> and pressure sensors,<sup>(12-18)</sup> used under the conditions of high-temperature, high-radiation, and chemically harsh environments, in which it is not possible to use conventional materials such as silicon (Si) and germanium (Ge).<sup>(19)</sup> Electrical characteristics and piezoresistive properties of the boron-doped (B-doped) p-type semiconducting CVD diamond films<sup>(12,15-18)</sup> and pressure sensor fabricated from the CVD diamond films<sup>(15-18)</sup> are reported in this paper.

## 2. CVD Growth of Diamond

B-doped CVD diamond films were deposited by a conventional microwave plasma CVD method.<sup>(7)</sup> The typical deposition conditions are listed in Table 1. The average growth rate of the B-doped polycrystalline diamond was about 0.3  $\mu\text{m}/\text{h}$ . The thickness of the deposited B-doped diamond film after 7 h growth was about 2  $\mu\text{m}$ .

It is known that the as-grown CVD diamond film exhibits a surface conductive layer whose conduction is p-type with very low mobility.<sup>(20,21)</sup> It is also reported that the electrical properties of heavily B-doped diamond films are dominated by impurity-band conduction with low mobility rather than by band conduction of holes.<sup>(22)</sup> Moreover, the electrical properties of the polycrystalline films, which consist of a columnar structure of diamond grains, are strongly affected by the grain boundaries. The hole mobility of the polycrystalline film is much lower than that of the single crystalline film.<sup>(16)</sup> The hole conduction in the surface conductive layer, the impurity-band conduction under high B-doping concentration, and the resistive conduction across the grain boundaries degrade the piezoresistive effect of the p-type CVD diamond film.

We carefully selected the deposition conditions for the p-type B-doped polycrystalline CVD diamond films to suppress these degradations. The as-grown diamond films were treated in an oxygen plasma for 3 min to remove the surface conductive layer after diamond CVD.<sup>(20,21)</sup> A B/C ratio of 1,000 ppm resulted in the required carrier concentration of  $\sim 10^{18} \text{ cm}^{-3}$  for suppression of the impurity-band conduction in the heavily B-doped diamond.

Table 1  
Deposition conditions of p-type CVD diamond film.

Method	microwave plasma CVD
Substrate	polycrystalline diamond/silicon wafer polycrystalline diamond wafer
Source gas	CO/H <sub>2</sub> /B <sub>2</sub> H <sub>6</sub>
Total gas flow	1 10 sccm
CO/H <sub>2</sub> ratio	1.8%
B/C ratio	1,000 ppm
Pressure	4,000 Pa
Microwave power	300 W
Substrate Temperature	900°C

An undoped polycrystalline diamond layer with a thickness of 20  $\mu\text{m}$  on a silicon wafer (poly-diamond/Si substrate) or an undoped polycrystalline diamond wafer with a thickness of 200  $\mu\text{m}$  (poly-diamond substrate) was used as a substrate for the deposition of B-doped CVD diamond films. The surface roughness of the polycrystalline diamond substrate was  $< 0.1 \mu\text{m}$ . Prior to the deposition, all substrates were cleaned in acid and then rinsed in deionized water. B-doped polycrystalline diamond films deposited on the polycrystalline diamond/Si substrates exhibited columnar structures of grains grown epitaxially on each diamond grains of substrate with low surface roughness. Homoepitaxial single-crystalline diamond film was also deposited on the high-pressure synthesized single-crystalline diamond (001) (HPSD) substrate in order to compare between single-crystalline and polycrystalline diamond films and to evaluate the grain boundary effect of polycrystalline films.

### 3. Electrical Properties of B-Doped CVD Diamond Films

The surface conductive layer of the as-deposited diamond film was removed by oxygen plasma treatment prior to the electrical measurements. Then a gold (Au)/titanium (Ti) double layer was deposited by electron beam evaporation as ohmic-contact electrodes for the B-doped diamond films. The electrical resistivity of the deposited p-type CVD diamond film was more than seven orders of magnitude smaller than that of the undoped diamond substrate:  $> 10^9 \Omega\cdot\text{cm}$ . The electrical resistivity  $\rho$ , hole concentration  $p$ , and Hall mobility  $\mu_h$  of the B-doped CVD diamond films were measured between 200 K and 455 K by the van der Pauw method and Hall effect measurement.

Figure 1 shows the electrical resistivity  $\rho$  plotted as a function of reciprocal temperature of the B-doped polycrystalline and single-crystalline diamond films deposited under the optimized conditions shown in Table 1. The activation energy  $\epsilon_A$  of the polycrystalline diamond film is 0.31–0.33 eV, the same as that of single-crystalline film, which agrees well with the reported value for boron acceptors in diamond.<sup>(2)</sup> The major carrier transports in these single- and polycrystalline CVD diamond films deposited under the optimized conditions are attributed to the band conduction of holes originating in B acceptors within the measured temperature range.

Figures 2 and 3 show the Hall mobility  $\mu_h$  and the hole concentration  $p$  of the B-doped polycrystalline and single-crystalline CVD diamond films as a function of reciprocal temperature.  $p$  of the polycrystalline and single-crystalline films are  $7 \times 10^{14} \text{ cm}^{-3}$  and  $1 \times 10^{15} \text{ cm}^{-3}$ , respectively, at 300 K. The hole concentrations of the B-doped polycrystalline and single-crystalline diamond films are almost the same within the measured temperature range. It is suggested that individual grains of the B-doped polycrystalline film exhibit the same qualities as the B-doped homoepitaxial single-crystalline diamond film. On the other hand,  $\mu_h$  of the polycrystalline film is  $36 \text{ cm}^2/\text{V}\cdot\text{s}$ , ten times smaller than that of the single-crystalline film at 300 K, because of the existence of the grain boundaries and/or the disordered crystalline orientation of diamond grains within the columnar structure. The diamond films deposited on the other substrates, such as fused quartz, exhibited a lower  $\epsilon_A$  (0.15 eV) and a lower  $\mu_h$  ( $< 1 \text{ cm}^2/\text{V}\cdot\text{s}$ ) than those deposited on diamond. The higher B-

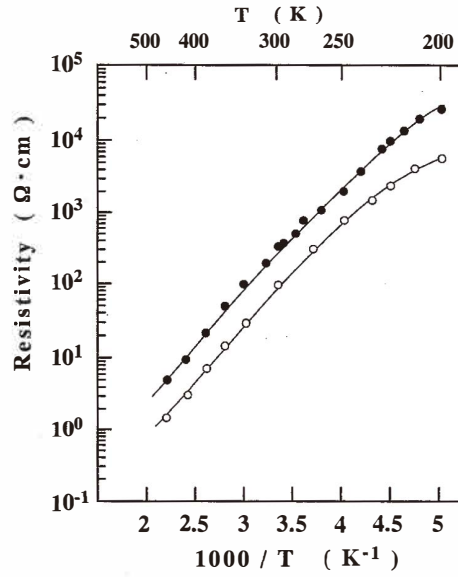


Fig. 1. Electrical resistivity  $\rho$  of the polycrystalline (●) and single-crystalline (○) B-doped CVD diamond films plotted as a function of reciprocal temperature.

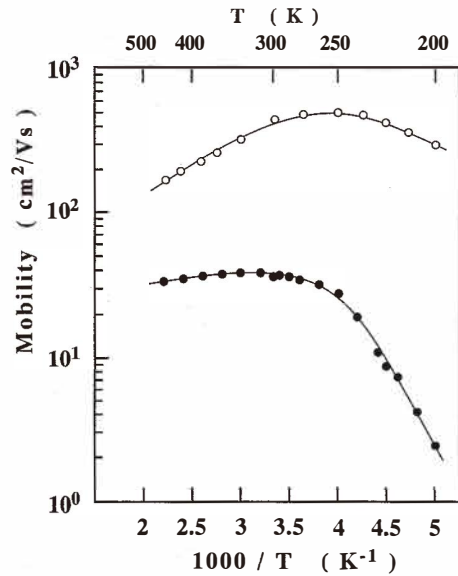


Fig. 2. Hall mobility  $\mu$  of the polycrystalline (●) and single-crystalline (○) B-doped CVD diamond films plotted as a function of reciprocal temperature.

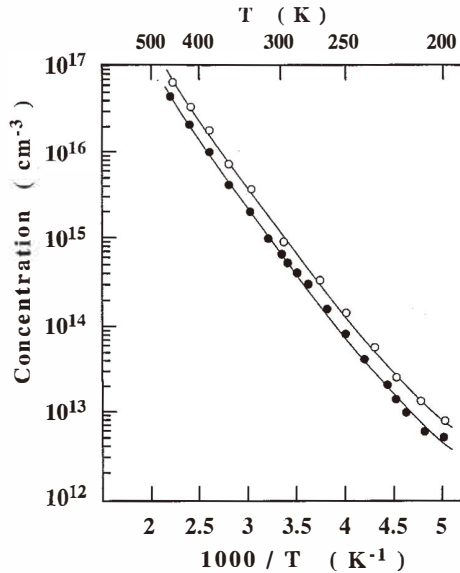


Fig. 3. Hole concentration  $p$  of the polycrystalline (●) and single-crystalline (○) B-doped CVD diamond films plotted as a function of reciprocal temperature.

doped ( $> 10^{19} \text{ cm}^{-3}$ ) CVD diamond film also showed a lower  $\epsilon_A (< 0.20 \text{ eV})$  and a lower  $\mu_h (< 10 \text{ cm}^2/\text{V}\cdot\text{s})$ .<sup>(20)</sup> Surface conductive layer of the as-grown CVD diamond film exhibited a lower  $\epsilon_A (0.05 \text{ eV})$  and a lower  $\mu_h (< 1 \text{ cm}^2/\text{V}\cdot\text{s})$ . It is confirmed that the hole conduction originated from the B acceptor with reasonably high mobility ( $> 30 \text{ cm}^2/\text{V}\cdot\text{s}$  at 300 K) was achieved in the polycrystalline diamond film under the optimized deposition conditions.

#### 4. Pressure Sensor Fabrication

The piezoresistive effect is the phenomenon whereby the electrical resistivity changes in response to an applied strain. It has mainly been investigated in semiconductors such as silicon (Si) and germanium (Ge).<sup>(19)</sup> The change in electrical resistivity originates from the change of valence band structures of p-type semiconducting materials by the strain.<sup>(23)</sup> The piezoresistors are usually fabricated on the diaphragm or cantilever structures in order to apply adequate strain to the piezoresistors. In the case of a circular diaphragm, the radial strain  $\epsilon_r(r)$  and the transverse strain  $\epsilon_t(r)$  on the diaphragm are calculated as

$$\epsilon_r(r) = \frac{3P}{8Et^2} \{a^2(1+\nu) - r^2(3+\nu)\} \quad (1)$$

$$\varepsilon_r(r) = \frac{3P}{8Et^2} \{a^2(1+\nu) - r^2(1+3\nu)\}, \quad (2)$$

where  $r$  is the distance from the center of the diaphragm,  $a$  and  $t$  are radius and thickness of the diaphragm,  $\nu$  and  $E$  are Poisson's ratio and Young's modulus of the diaphragm materials, respectively.  $P$  is the pressure difference between upper and lower surface of the diaphragm. The  $\varepsilon_r(r)$  and  $\varepsilon_t(r)$  take the same maximum value at the center of the diaphragm ( $r = 0$ ) as

$$\varepsilon_r(0) = \varepsilon_t(0) = \frac{3a^2(1+\nu)}{8Et^2} P. \quad (3)$$

Gauge factor  $K$ , an index of the sensitivity of a piezoresistive sensor material, is defined as the value of relative change in electrical resistance ( $\Delta R/R_0$ ) divided by the applied strain  $\varepsilon$ ;

$$K = \frac{\Delta R/R_0}{\Delta L/L_0} = \frac{\Delta R/R_0}{\varepsilon}, \quad (4)$$

where  $\Delta L/L_0$  is the relative change in piezoresistor length.  $\Delta R/R_0$  of the piezoresistor as a function of the applied strain  $\varepsilon$  can be divided into two terms as

$$\Delta R/R_0 = (1+2\nu)\varepsilon + \Delta\rho/\rho_0, \quad (5)$$

where  $(1+2\nu)\varepsilon$  is due to the geometrical deformation of the piezoresistor and  $(\Delta\rho/\rho_0)$  is due to the electrical resistivity change of the piezoresistor materials. The piezoresistive effect for semiconducting materials is mainly dominated by the term  $(\Delta\rho/\rho_0)$ . The  $K$  value of p-type crystalline Si is approximately 150.<sup>(15)</sup> It was also reported that  $K$  values of B-doped p-type polycrystalline and homoepitaxial single crystalline CVD diamond films were 6–1,000 and  $> 550$ , respectively, at room temperature on the diaphragm or cantilever configuration.<sup>(12–18,24,25)</sup>

The CVD diamond piezoresistors were fabricated from B-doped polycrystalline diamond film grown on the flat insulating polycrystalline diamond substrate using the reactive ion etching technique. Under the diamond piezoresistor, the diaphragm structure was formed by etching the substrate from the back. Typical steps of the fabrication process are illustrated in Fig. 4. After the deposition of the B-doped diamond films, the 3- $\mu\text{m}$ -thick aluminum (Al) film is evaporated onto the diamond film. The Al film is patterned and used as the mask for the diamond-film etching process. The B-doped diamond film is etched by reactive ion etching (RIE) in oxygen plasma. RF power and pressure of the typical RIE etching conditions are 150 W and 5.3 Pa, respectively. The etching rate of the diamond layer is about 2  $\mu\text{m}/\text{h}$ , which is four times higher than that of the Al mask film. The length and width of the fabricated diamond piezoresistor are 500  $\mu\text{m}$  and 50  $\mu\text{m}$ , respectively. Then the Au/Ti ohmic electrodes for the piezoresistor are deposited. Under the diamond piezoresistor, a circular diaphragm structure is further fabricated by etching a portion of the Si substrate from the back. Diameter and thickness of the diaphragm are 2 mm and 400  $\mu\text{m}$ ,

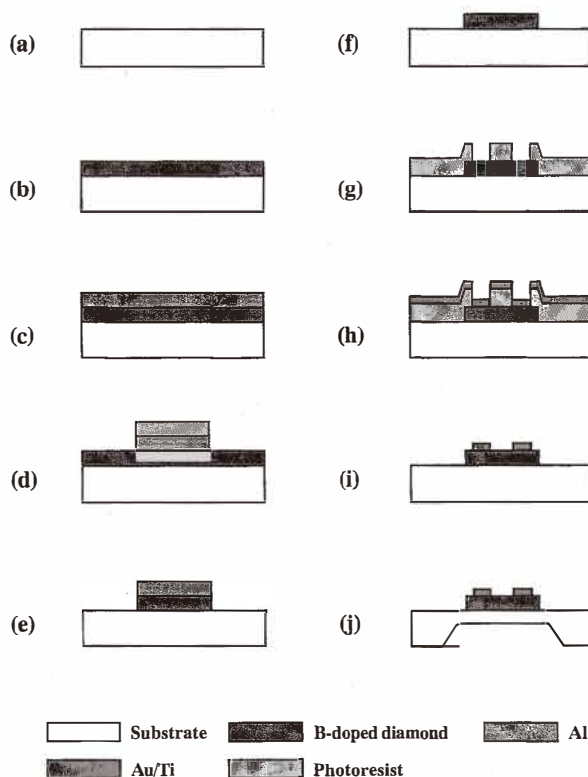


Fig. 4. Typical steps of fabrication process for the diamond piezoresistor on the diaphragm structure. (a) Cleaning of substrate; (b) deposition of B-doped CVD diamond film; (c) evaporation of Al film; (d) etching and patterning of Al film; (e) etching of B-doped diamond layer by RIE process; (f) removal of Al mask; (g) patterning of photoresist layer; (h) evaporation of Au/Ti layer; (i) lift-off; (j) fabrication of diaphragm structure.

respectively. The overview of the diamond piezoresistor device and the scanning electron microscope (SEM) image of the diamond piezoresistor rod are shown in Figs. 5 and 6, respectively. Each individual piezoresistor was isolated by the electrical resistance of more than  $10\text{ G}\Omega$ .

## 5. Piezoresistive Properties of B-Doped CVD Diamond Films

The B-doped diamond piezoresistors on the diaphragm were set in the gas pressure system as shown in Fig. 7(a). Ar gas pressure (0–10 Mpa) was applied to the piezoresistor on the fabricated diamond/Si diaphragm in the gas pressure system. The whole system



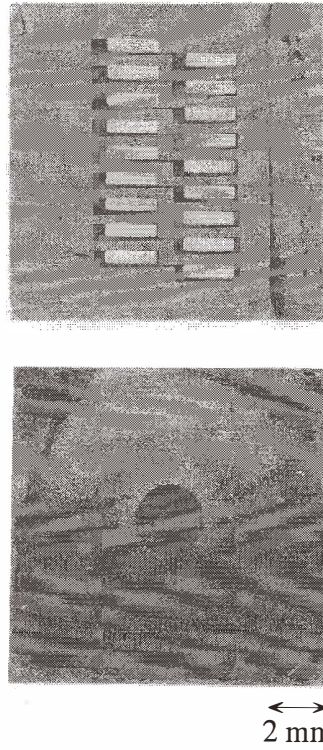


Fig. 5. Overview of the diamond piezoresistor device.

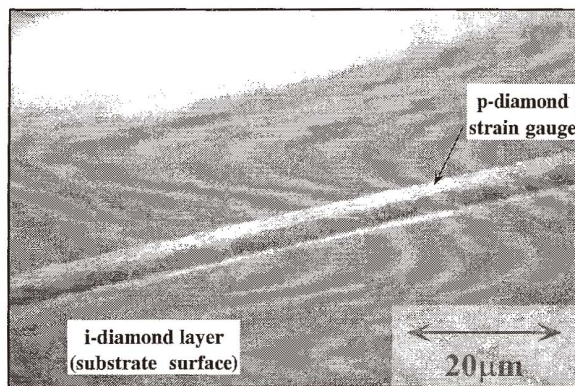


Fig. 6. SEM projection image of the diamond piezoresistor rod.



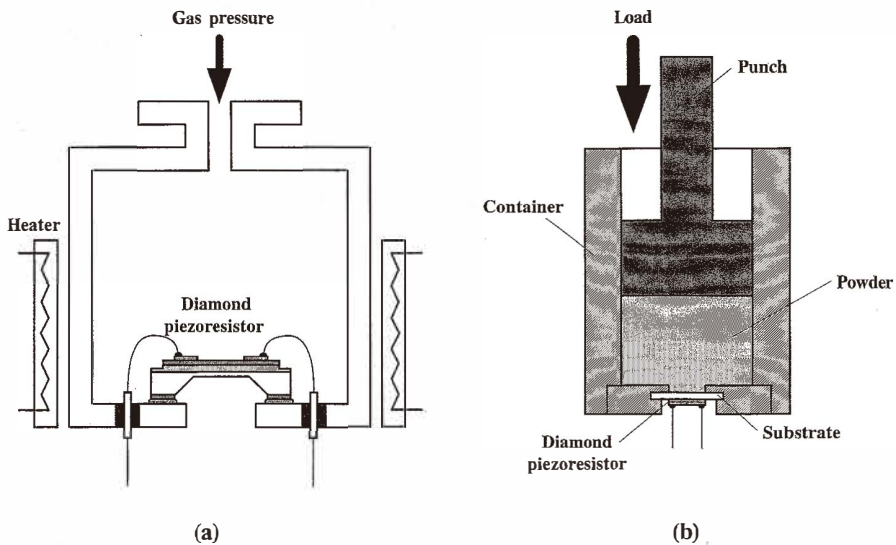


Fig. 7. Schematic illustrations of the application systems of the CVD diamond piezoresistors: (a) gas pressure system; and (b) powder compaction system.

could be heated up to 200°C. In another application, the piezoresistor on the insulating diamond wafer was fixed on the bore at the bottom of container in the powder compaction system as shown in Fig. 7(b). Then iron powder with a particle size of about 100  $\mu\text{m}$  diameter was charged in the container. The pressure was applied to the reverse side of the piezoresistor device through the bore by loading a punch.

Figure 8 shows the relative change in the electrical resistance ( $-\Delta R/R_0$ ) of the p-type polycrystalline CVD diamond piezoresistor as a function of pressure  $P$  applied to the diamond/Si diaphragm using the gas pressure system (Fig. 7(a)) at different temperatures. The  $R$  of the piezoresistor decreases with increasing compressive stress applied to the piezoresistor as shown in Fig. 8. The slope of  $-\Delta R/R_0$  versus  $P$  is about 0.30% per 1 MPa at room temperature and about 0.25% per 1 MPa at 200°C. The gauge factor  $K$  for this piezoresistor was calculated using eqs. (3) and (4) neglecting the effect of transverse strain. Figure 9 shows the  $K$  for the p-type polycrystalline CVD diamond piezoresistor calculated at different strains  $\varepsilon$  as a function of temperature. The  $K$  is about 1000 at room temperature, which is 6 times larger than that of Si. Though the  $K$  decreases with elevating temperature, it remains above 700 even at 200°C. The p-type diamond piezoresistor has the potential to operate under high-temperature ( $> 200^\circ\text{C}$ ) and high-pressure ( $> 10$  MPa) environments.

Figure 10 shows the  $\Delta R/R_0$  of the p-type diamond piezoresistor on the insulating diamond wafer (Fig. 7(b)) at room temperature as a function of load applied to the punch. The  $R$  of the piezoresistor increased with increasing load force, since the force was applied from the back of the diamond wafer. The  $\Delta R/R_0$  was proportional to the applied load as shown in Fig. 10 up to 500 kgW.

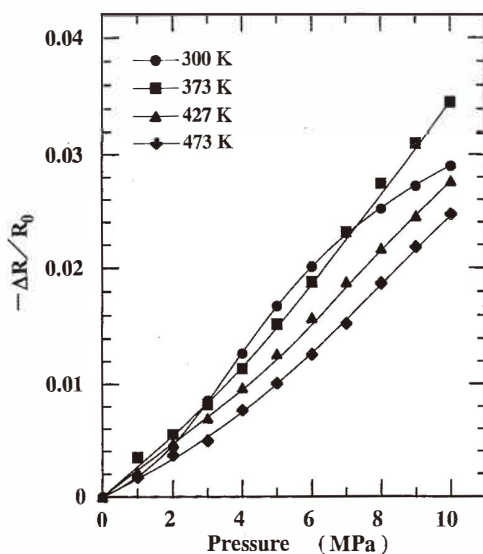


Fig. 8. Relative change in the electrical resistance ( $-\Delta R/R_0$ ) of the p-type diamond piezoresistor shown in Fig. 7(a) as a function of pressure  $P$  applied to the diamond/Si diaphragm at different temperatures: ● 27°C; ■ 100°C; ▲ 150°C; ◆ 200°C.

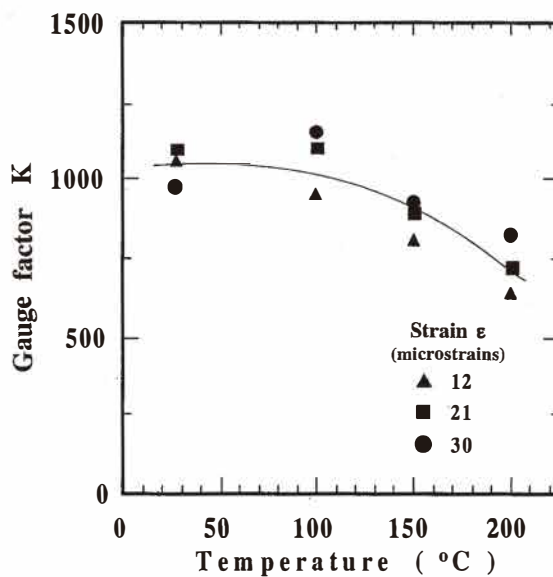


Fig. 9. Gauge factors  $K$  for the p-type diamond piezoresistor shown in Fig. 7(a) as a function of temperature at different strains: ▲ 12 microstrains; ■ 21 microstrains; ● 30 microstrains.

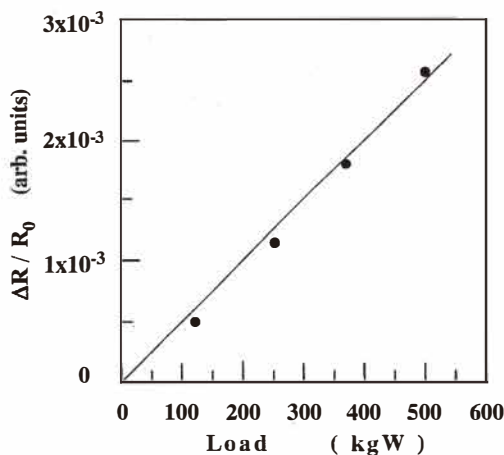


Fig. 10. Relative change in the electrical resistance  $\Delta R/R_0$  of the p-type diamond piezoresistor shown in Fig. 7(b) at room temperature as a function of applied load.

## 6. Summary

Boron-doped p-type polycrystalline CVD diamond films were grown on flat undoped polycrystalline diamond substrates under the optimized conditions to suppress degradations originating from the surface conductive layer, grain boundaries, and impurity band conduction. Piezoresistors of the optimized p-type polycrystalline diamond film were fabricated on the diaphragm structure using photolithography and reactive ion etching in oxygen plasma. A large piezoresistive effect is observed in the optimized p-type diamond piezoresistor. The gauge factors  $K$  for the p-type diamond piezoresistor are calculated to be  $\sim 1,000$  at room temperature and  $> 700$  at  $200^\circ\text{C}$ .

## Acknowledgment

Part of this work was conducted in the program; "Advanced Chemical Processing Technology," consigned to ACTA from NEDO, which was carried out under the Industrial Science and Technology Frontier Program enforced by the Agency of Industrial Science and Technology.

## References

- 1 G. A. Baraff: Phys. Rev. A **26** (1964) 133.
- 2 A. T. Collins and A. W. S. Williams: J. Phys. C, Solid State Phys. **4** (1971) 1789.
- 3 J. E. Graebner, M. E. Reis, L. Seibles, T. M. Hartnett, R. P. Miller and C. J. Robinson: Phys. Rev. B **70** (1994) 3702.

- 4 H. J. Mcskimin and P. Andreatch: J. Appl. Phys. **43** (1972) 2944.
- 5 B. V. Spitsyn, L. L. Boilov and B. V. Derjaguin: J. Cryst. Growth **52** (1981) 219.
- 6 S. Matsumoto, Y. Sato, M. Kamo and N. Setaka: Jpn. J. Appl. Phys. **21** (1982) L183.
- 7 M. Kamo, Y. Sato, S. Matsumoto and N. Setaka: J. Cryst. Growth **62** (1983) 642.
- 8 D. R. Kania, M. I. Landskrass, M. A. Plano, L. S. Pan and S. Han: Diamond Relat. Mater. **2** (1993) 1012.
- 9 L. S. Pan, P. Pianrta, D. R. Kania, O. L. Landon, K. V. Ravi and L. S. Plano: Proc. 1st Int. Symp. on Diamond and Diamond-like Films (1990) 424.
- 10 J. P. Bade, S. R. Sahaide, B. R. Stoner, J. A. Von Windheim, J. T. Glass, K. Miyata, K. Nishimura and K. Kobashi: Diamond Relat. Mater. **2** (1993) 816.
- 11 J. G. Ran, C. Q. Zheng, J. Ren and M. Hong: Diamond Relat. Mater. **2** (1993) 793.
- 12 M. Aslam, I. Taher and A. Masood: Appl. Phys. Lett. **60** (1992) 2923.
- 13 I. Taher, M. Aslam, M. A. Tamor, T. J. Potter and R. C. Elder: Sensors and Actuators A **45** (1994) 35.
- 14 J. L. Davidson, D. R. Wur, W. P. Kang, D. L. Kinser and D. V. Kerns: Diamond Relat. Mater. **5** (1996) 86.
- 15 M. Deguchi, M. Kitabatake, T. Hirao: Proceedings of 6th European Conference on Diamond, Diamond-like and Related Materials 1995, Diamond and Related Materials **5** (1996) 728.
- 16 M. Deguchi, M. Kitabatake, T. Hirao: Thin Solid Films **281–282** (1996) 267.
- 17 M. Deguchi, N. Hase, M. Kitabatake, H. Kotera, S. Shima, H. Sakakima: Diamond Films and Technology **6** (1996) 77.
- 18 M. Deguchi, N. Hase, M. Kitabatake, H. Kotera, S. Shima, M. Kitagawa: Diamond and Related Materials **6** (1997) 367.
- 19 C. S. Smith: Phys. Rev. **94** (1954) 42.
- 20 M. Deguchi, Y. Mori, N. Eimori, Y. Show, M. Kitabatake, A. Hatta, T. Ito, A. Hiraki, T. Izumi and T. Hirao: Proc. 2nd Int. Conf. on Application of Diamond Films and Related Materials (MYU, Tokyo, 1993) p. 793.
- 21 H. Nakahata, T. Imai and N. Fujimori: Proc. 2nd Int. Symp. on Diamond Materials 91–8 (The Chemical Society, New Jersey, 1991) p. 487.
- 22 M. Werner: Phys. Stat. Sol. (a) **154** (1996) 385.
- 23 Y. Kanda: Sensors and Actuators A **28** (1991) 83.
- 24 W. Wanlu, X. Jiang and C. P. Klages: Chinese Science Bull. **40** (1995) 209.
- 25 O. Dorsch, K. Holzner, M. Werner and E. Obermeier: Diamond Relat. Mater. **2** (1993) 1096.

### About the Authors

**Makoto Kitabatake** was born in Fukushima, Japan, in 1956. He received a B.S., an M.S. and a D.S. degree in Engineering from Tohoku University, Sendai, Japan, in 1978, 1980 and 1988, respectively. In 1980 he joined Matsushita Electric Industrial Co. Ltd. At present he is a senior researcher in the Central Research Laboratories. He is involved in the studies on thin film science and technology especially for new diamond materials such as diamond and silicon carbide.

**Masahiro Deguchi** was born in Kyoto, Japan, in 1963. He received a B.S. and an M.S. degree in Electrical Engineering from Osaka University, Osaka, Japan, in 1986 and 1988, respectively. In 1988 he joined Matsushita Electric Industrial Co. Ltd. At present he is a senior researcher in the Central Research Laboratories. He mainly conducts researches on chemical vapor deposition technique of new diamond material such as diamond and silicon carbide.